Supplementary Material

Supplementary Figure Legends

Supplementary Figure S1: (A) Formation of functional synapses in hippocampal neurons. 13 DIV neurons were immunostained for the postsynaptic marker PSD95 and the presynaptic marker Synapsin I (left image). 12 DIV neurons were transfected with RFP-PSD95, fixed and immunostained for Synapsin I (right image) 1 day later. Insets show enlargements of dendritic segments where most PSD clusters are adjacent to Synapsin I puncta. **(B) Dendritic mRNAs localize in distinct RNPs under several conditions of synaptic activity.** *MAP2*/*CaMKIIα*, *MAP2*/*β-actin* or *CaMKIIα*/*β-actin* pairs were detected by double ISH. Quantification of signal colocalization in dendrites of 7-8 DIV, 14-16 DIV, 15 DIV and 21-23 DIV hippocampal neurons in standard medium or 15 DIV neurons treated with DHPG, glutamate or a silencing cocktail of APV, TTX and CNQX. Error bars represent the SEM of colocalization rates in individual dendrites. 45, 30, 19, 36, 57, 49, 40, 118, 77, 68, 45, 37, 51, 23, 65, 37, 36, 38, 25, 51 or 61 dendrites were analyzed for each respective condition (in the order they appear on the graph). There were no significant differences between the six groups for each pair as a whole (ANOVA). When comparing each condition to the control, however, glutamate treatment resulted in a significant increase in colocalization between *MAP2* and *β-actin* (Student's t-test, * $p<0.05$). (**C**) **Efficiency of double ISH with probes targeting two different mRNAs**. Number of observed particles of *CaMKIIa*, *MAP2* or *β-actin* mRNAs when each mRNA was detected first (blue) or second (red) in double ISH experiments. Values are normalized to particle numbers obtained when the respective mRNAs were detected first. 38, 35, 21, 22, 27 or 22 dendrites were analyzed for each respective

condition (with the order they appear on the graph). (**D**) **Efficiency of double ISH with non-overlapping probes targeting the same mRNA.** Number of observed particles of *CaMKIIa*, *MAP2* or *β-actin* mRNAs when non-overlapping probes were detected first (blue) or second (red) in double ISH experiments. Values are normalized to particle numbers obtained with the first detection. The numbers of analyzed dendrites were 26, 24 and 29, respectively. In (**C**) and (**D**), error bars represent the SEM (normalized) of particle numbers in individual dendrites. **(E) Double detection of *CaMKIIa* and *MAP2* mRNAs using the MS2 system followed by ISH.** Hippocampal neurons were co-transfected with *CaMKIIa* 3'-UTR-24xMS2 and MCP-YFP. *MAP2* mRNA detected by ISH and *CaMKIIa* mRNA detected with anti-GFP, show a low degree of colocalization in dendrites (n=19) of hippocampal neurons. Images represent adjacent regions of one representative dendrite. Detection of YFP tagged *CaMKIIa* mRNA by ISH is used as a positive control of colocalization (n=9). Error bars represent the SEM of colocalization rates in individual dendrites. * $p<0.05$, *** $p<0.001$.

Supplementary Figure S2: (**A**) **Efficiency of single ISH experiments.** *MAP2* mRNA was hybridized with DIG-labeled probe in the absence (1, n=33) or presence of equal amounts of overlapping cold (3, n=32), overlapping FL-labeled (4, n=47) or non-overlapping DIG-labeled (2, n=57) probe and detected with anti-DIG-peroxidase (POD) (blue). *MAP2* mRNA was hybridized with FL-labeled probe in the absence (1', n=37) or presence of equal amounts of overlapping cold (3', n=28), overlapping DIG-labeled (4', n=35) or non-overlapping FL-labeled (2', n=44) probe and detected with anti-FL-POD (red). All values are normalized to particle numbers obtained with DIG-labeled probe detected by anti-DIG-POD (1, blue). Error bars represent the SEM

(normalized) of particle numbers in individual dendrites. N represents number of analyzed dendrites. 1, 1', 2 and 2' were all significantly different from 3, 3', 4 and 4' (*** $p<0.001$). There were no statistically significant differences within these two groups. (**B**) **Control competition assay.** *MAP2* RNA was detected in the absence or presence of 5-fold excess of cold probe against *CaMKII*α. **(C) Efficiency of hybridization and detection.** Average cell body intensities (left) and dendritic particle intensities (right) for *MAP2* when one DIG labeled probe or two non-overlapping DIG labeled probes are used, normalized to one probe. In 4 independent experiments, at least 100 cell bodies and 3000 dendritic particles were measured in total per condition. Error bars represent the SEM of the average values of the individual experiments. (**D**) **Detection is linear over a wide range of DIG concentrations**. Average cell body intensities (left) and dendritic particle intensities (right) for *MAP2* detected with probes synthesized using different concentrations of DIG-UTP in the NTP mix (1 mM, 2 mM, 3.5 mM (standard concentration used in all experiments), 5 mM, 6.5 mM out of 10 mM total UTP), normalized to the standard concentration (3.5 mM). In 4 independent experiments, 100-180 cell bodies and 2200-5100 dendritic particles were measured in total per condition. Error bars represent the SEM of the average values of the individual experiments. Number of *MAP2* particles (bottom) detected with 1 mM, 3.5 mM or 6.5 mM DIG-UTP, normalized to 3.5 mM. 44, 55 or 44 dendrites were analyzed. Error bars represent the SEM of number of particles in individual dendrites. (**E**) **Single particle intensities**. Frequency distribution of dendritic *MAP2* particle intensities (n=1300). Values were normalized to the average particle intensity. Red dashed lines represent the intensities expected for particles containing 1, 2 (asterisk, corresponding to the average intensity of a dendritic particle), 3 and 4 molecules, respectively, based on the results of the

competition assay. **(F) Competition assay for *Septin7*.** *Septin7* RNA was detected in the absence or presence of equal amounts of cold probe in hippocampal neurons.

Supplementary Figure S3: (A) Nuclear staining for *β-actin* is present in Stau2 depleted and control neurons, but absent after actinomycin D (ActD) treatment. *β-actin* was detected in wild type (untransfected) or Stau2-deficient hippocampal neurons (transfected with shStau2 and co-expressing EGFP, marked with asterisks) which were treated with actinomycin D for t=0 or t=4h. Nuclear *β-actin* signal is similar between transfected and untransfected neurons and is absent in neurons treated with ActD for 4h. **(B) Stau2 affects the stability of *MAP2* and *β-actin*.** Average intensity of *MAP2* and *β-actin* signal in the cell body of hippocampal neurons which were transfected with shStau2 or misStau2 and treated for t=0 (blue) or t=4h (red) with actinomycin D. Intensities are first normalized to untransfected neurons from the respective sample and then to the control (t=0) for each condition. Error bars represent SEM of cell body intensities of individual cells. 81, 72, 23, 26, 149, 145, 44 or 84 cells were analyzed for each respective condition (with the order they appear on the graph). **(C) Stau2 affects the composition of *MAP2* but not *β-actin* RNPs.** Number of detected particles of *MAP2* and *β-actin* RNAs in the presence (red) or absence (blue) of equal amounts of cold probe in control (untransfected or transfected with misStau2) or Stau2-deficient (transfected with shStau2) hippocampal neurons. Numbers of detected particles are normalized to the respective labeled:cold 1:0 condition. Error bars represent the SEM of particle numbers in individual dendrites. 66, 65, 41, 16, 93, 132, 29, 39, 28, 32, 57 or 40 dendrites were analyzed for each respective condition (with the order they appear on the graph). (**D**) **Stau2 does not affect colocalization of dendritic mRNAs in RNPs.** *MAP2*/*CaMKIIα* or *MAP2/β-*

actin pairs were detected by double ISH in wild type (untransfected) or Stau2-deficient hippocampal neurons (transfected with shStau2, expressing EGFP as a marker). Error bars represent the SEM of colocalization rates in individual dendrites. 45, 19, 118 and 23 dendrites were analyzed for each respective condition (with the order they appear on the graph). In (**B**), (**C**) and (**D**), asterisks denote statistical significance as determined using two-tailed Student's t-test for the complete data set. *$p<0.05$, ** $p<0.01$, *** $p<0.001$. **(E) Reduction of Stau2 levels in shStau2 transfected neurons.** shStau2 transfected hippocampal neurons (expressing EGFP as a marker, asterisk) were fixed and immunostained with anti-Stau2. Untransfected neurons shown have much higher levels of Stau2, glia (cell in the middle) show background staining.

Supp. Figure 1, Mikl et al

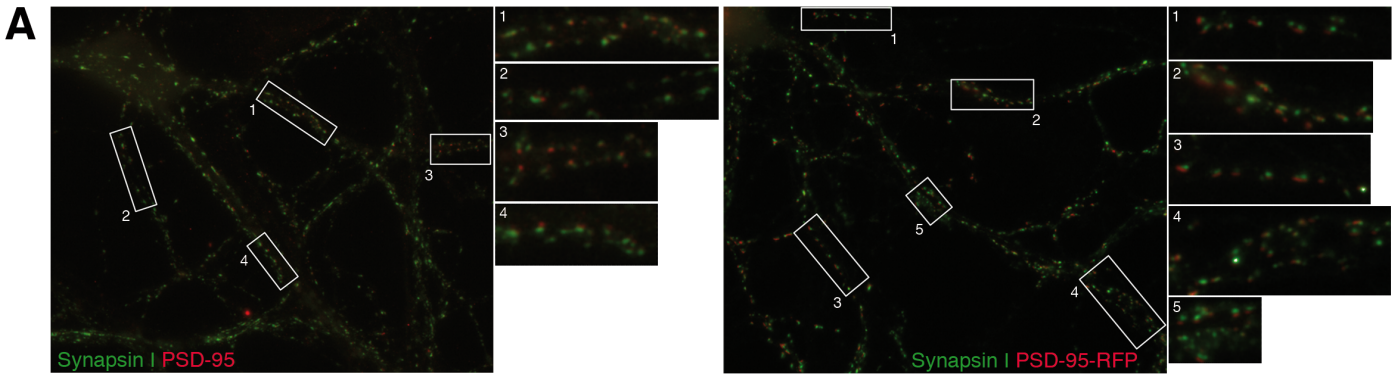

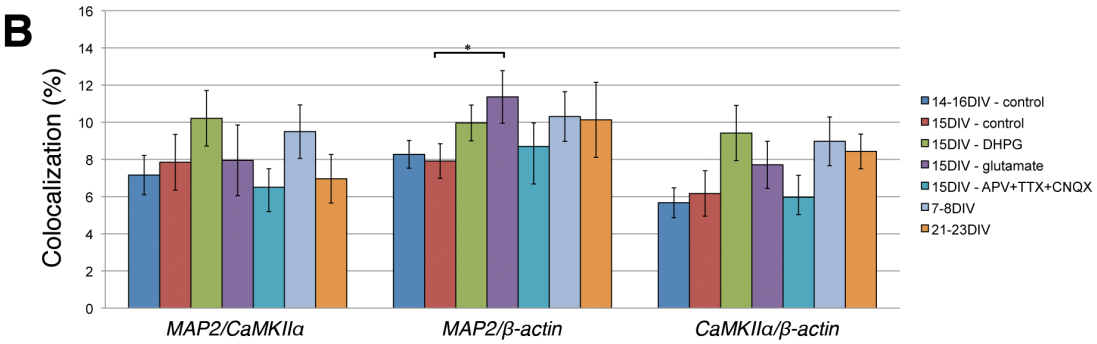

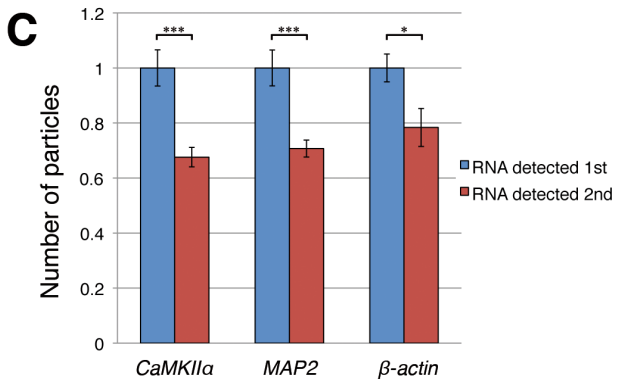

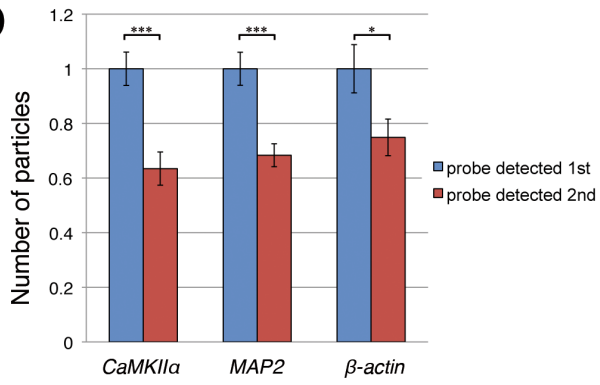

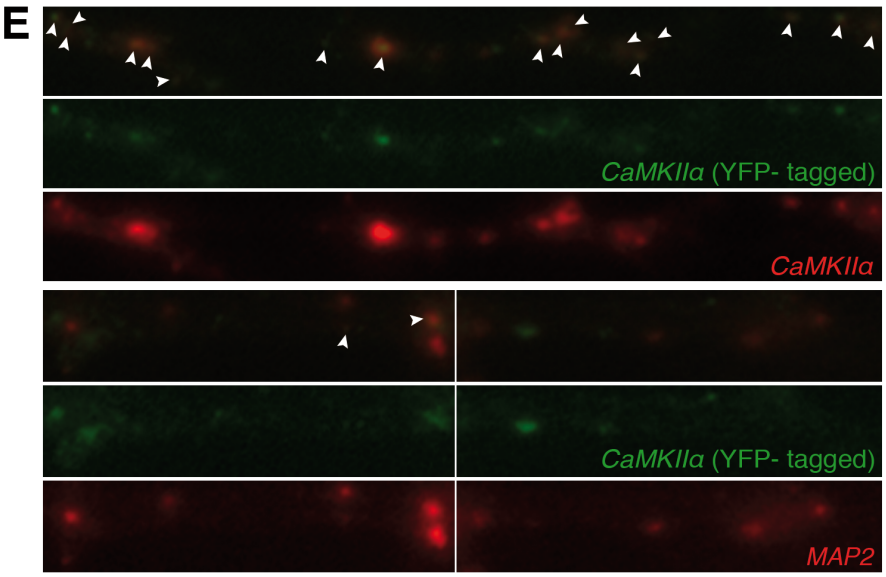

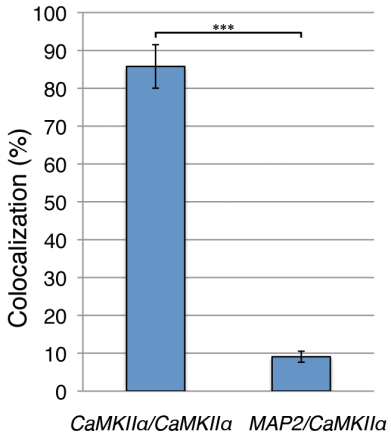

Supp. Figure 2, Mikl et al

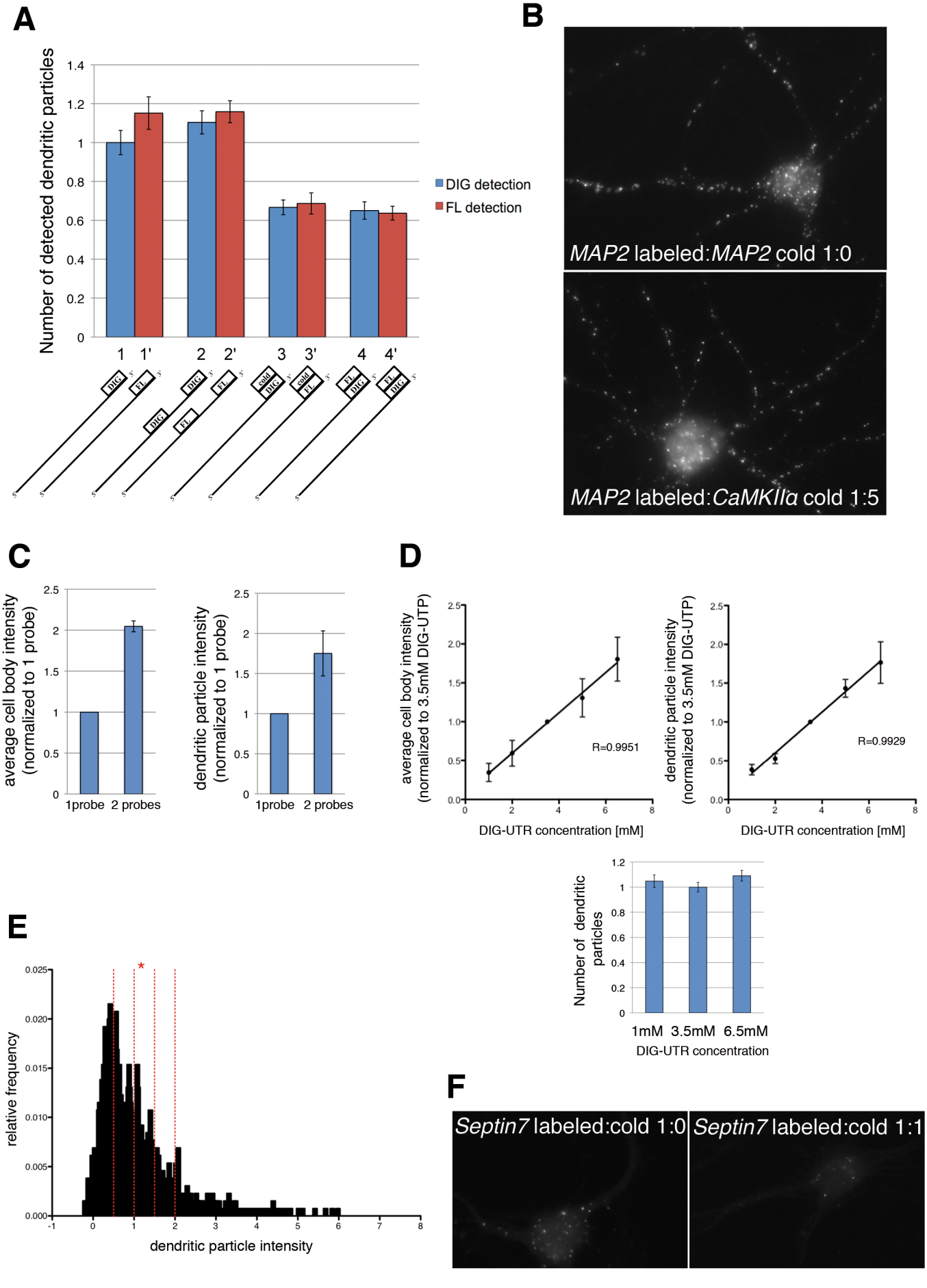

Supp. Figure 3, Mikl et al

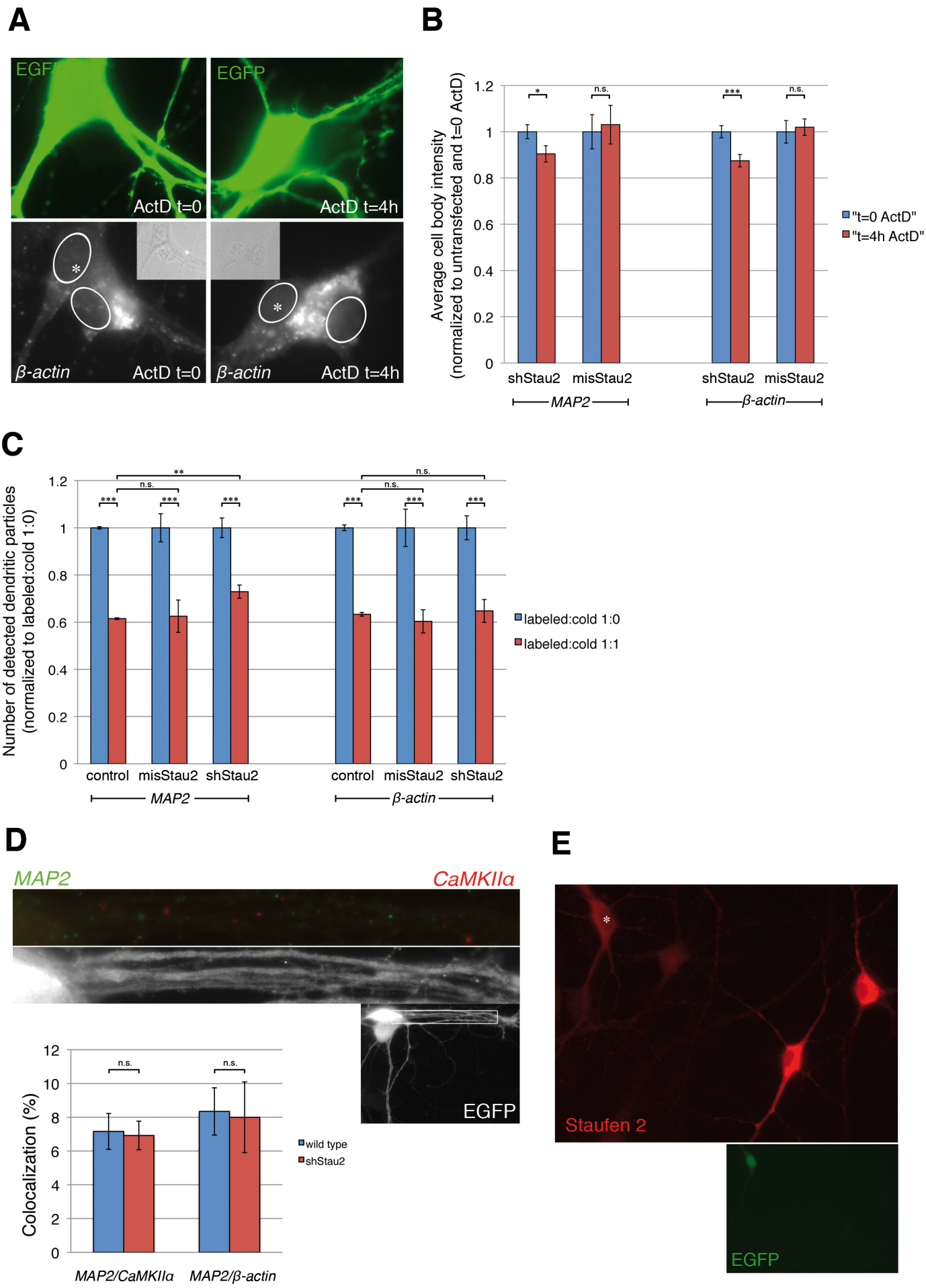

Supplementary Methods

Neuronal cultures, transfections and pharmacological treatments: Hippocampal neurons from embryonic day 17 rats were prepared as described previously (Goetze *et al*, 2004) and used at 14-16 DIV, unless stated otherwise. 14-16 DIV neurons form networks, functional synaptic contacts (Goetze *et al*, 2006), show synaptically-driven spontaneous activity, as demonstrated by Ca^{2+}-oscillations, membrane potential recordings and receptor blockage experiments (Bacci *et al*, 1999) and have mature spines (Papa *et al*, 1995; Yuste & Bonhoeffer, 2001), although their density and morphology changes with age. Immunostainings against Synapsin I, PSD-95 (**Supplementary Fig S1A**), Synaptophysin or Homer (not shown), demonstrate that 13 DIV hippocampal neurons express pre- and postsynaptic proteins. Moreover, most PSD95 puncta - endogenous or RFP fusions (**Supplementary Figure 1A**) - were found in close contact with Synapsin I-positive spots, indicating that dendritic spines receive normal presynaptic inputs. Hippocampal neurons were transfected with PSD-95-RFP at 12 DIV and stained with anti-Synapsin I 1 day later. To down-regulate Stau2, 11 DIV neurons were transfected as described before (Goetze *et al*, 2006) with a pSuperior plasmid co-expressing an shRNA targeting Stau2 (si2-2) or a mismatch shRNA together with EGFP to identify transfected cells. 15 DIV neurons were treated with 50 µM DHPG (Tocris) for 15min, 10 µM glutamate for 2min or a cocktail of 1 µM TTX (Na_v channel blocker), 50 µM APV (NMDA-R antagonist) and 100 µM CNQX (AMPAR/kainate-R antagonist) overnight (all Sigma), as described earlier (Dictenberg *et al*, 2008; Zeitelhofer *et al*, 2008).

Constructs: The following sequences, as PCR products or cloned into pBluescript II KS+, SK+ or pGEM-T served as templates for ISH probes: MAP2 (U30938 [GenBank], nucleotides 181-1340 and 2532-3738, 1st and 3rd third of the 3'-UTR), CaMKIIα (NM_177407, 1616-3117 and 3156-4756, 1st and 2nd half of the 3'-UTR), GAPDH (M17701, 4-1233), Tubulin α3 (NM_001040008, 420-1069, provided by J. Deshler), Tubulin β4 (750bp, provided by O. Steward), Septin7 (NM_022616, 11-1490) and β-actin (NM_031144, 21-520, 221-740 and 723-1240).

The following plasmids were used for transfections: PSD-95-RFP and PSD-95-GFP (generous gifts from D. Bredt), pSuperior (Oligoengine) expressing shStau2 or misStau2 (Goetze *et al*, 2006). pmax-NLS80-MCP-YFP was a generous gift from K. Czaplinski (Stony Brook). RSV-lacZ-24xMS2-CaMKIIα 3'-UTR was generated by replacement of the 8xMS2 of RSV-lacZMS2bs-CaMKIIα 3'-UTR (Rook *et al*, 2000) with 24xMS2 (from pSL-MS2-24X, kindly provided by Rob Singer, Albert Einstein College of Medicine).

Antibodies: GFP, EGFP and YFP were detected with an anti-GFP antibody (kindly provided by W. Sieghart, CBR, MUW). Synaptic proteins were detected with mouse monoclonal anti-PSD-95 (1:200, ABR), mouse monoclonal anti-Synaptophysin (1:1000, Roche), rabbit anti-Synapsin I (1:1000, Millipore) and rat polyclonal anti-Homer (1:500, Serotec). The following secondary antibodies were used: donkey anti-rabbit Alexa488, goat anti-rat Alexa568 (Invitrogen) and goat anti-mouse Cy3 (Dianova), all at 1:1000.

Double ISH: Only particles that did not appear out of focus were taken into account and crowded compartments like dendritic bifurcations were omitted. For 1, 2 or 3

RNA molecules per particle, colocalization rates of 0%, 66.7% and 85.7%, respectively, can be expected for competing probes. In the data presented in **Fig. 2**, 27% to 52% (relative, normalized to the condition of non-overlapping target sequences) of the particles were recognized by both probes.

ISH competition assay: For quantification of particle numbers, dendritic puncta in a region 10-75µm from the cell body were counted manually. From at least three different experiments, particle numbers for individual dendrites for all three conditions (1:0, 1:1, 1:3) were normalized to the average particle numbers of the 1:0 condition of the respective experiment. For quantification of particle intensities, images for all three conditions of an experiment were thresholded equally and total signal intensity for every dendritic particle between 10 and 75 µm from the cell body was measured using Metamorph. The individual values were normalized to the average total particle intensity in the 1:0 condition of the respective experiment and combined for all three experiments. Expected particle numbers and intensities for different concentrations of cold probe and different numbers of RNA molecules per particle were calculated based on the probability of binding of labeled or cold probe. For particle numbers, the following formula was used: $x=1-(k/(k+1))^n$ (x=relative particle numbers, k=ratio cold/labeled probe, n=number of molecules per particle). As control, a 5-fold excess of cold probe targeting a different sequence was added.

ISH efficiency controls: Several probes were tested for each mRNA and those that performed better (detecting a higher number of particles in dendrites, probably due to higher accessibility to the target) were used. Moreover, adding another, identically labeled, non-overlapping probe in the hybridization mix did not result in a significant

increase in the number of detected particles (**Supplementary Fig S2A**), arguing for high efficiency of the selected probes. Importantly, the addition of the second probe resulted in a 75% increase of average particle intensity (as well as the expected change of distribution of intensities). This value approaches the 82% increase that is expected (based on the relative number of UTPs and consequently the relative amount of incorporated DIG of the two probes) when all molecules are bound by both probes (**Supplementary Fig S2C)**, suggesting that the efficiency of hybridization and detection is indeed high. Calibration experiments, where we used 1mM, 2mM, 3.5mM (standard concentration used in all experiments), 5mM or 6.5mM DIG-UTP (out of 10mM total UTP in the reaction mix), demonstrated that the detection is linear over a wide range (**Supplementary Fig S2D,** top), as the mean and distribution of particle intensities changed proportionally. Reduction of the concentration of DIG-UTP did not result in a decrease in the number of detected particles, confirming the sensitivity of the standard protocol (**Supplementary Fig S2D,** bottom).

ISH on Stau2-deficient neurons: 3 days after transfection, cells were fixed for RNA detection by ISH combined with detection of EGFP using an anti-GFP antibody. Average fluorescence intensity of the ISH signal in the cell body of transfected cells was quantified from comparable focal planes (where dendritic particles are in focus) using Metamorph. Intensities of dendritic *β-actin, Septin7*, *CaMKIIa* and *MAP2* RNA particles were obtained as described above and dendritic background fluorescence was subtracted to account for any effects of modest bleed-through resulting from very high levels of EGFP. For all analyses, ISH signal in transfected cells was compared to untransfected cells on the same glass coverslip to account for possible differences in

detection. Subsequently, we normalized the values for shStau2-expressing to mismatch transfected cells from the same experiment.

The stability assay was performed as follows: 3 days after transfection with shStau2 and misStau2, neurons were treated with 6 µg/µl actinomycin D (Sigma) and fixed for ISH at t=0 or t=4h. Average cell body intensities were measured in transfected and untransfected cells and the values were normalized first to untransfected cells on the respective glass coverslip to account for the general effect of actinomycin D treatment. To determine the specific effect of actinomycin D treatment on transfected cells, values were then normalized to the respective control (t=0) for both conditions (shStau2 and misStau2). 4 independent experiments yielded the same outcome.

Imaging: Images were acquired using a 63x planApo oil immersion objective, 1.40 NA, an Axioplan microscope (both Zeiss) equipped with an F-view II CCD camera and AnalysisB software (both Olympus). The same acquisition settings were used for all conditions of one experiment. Usually a single frame focusing on distal dendritic particles was acquired. Selected colocalization experiments (parts of **Fig. 1** and **Fig. 2**) were also imaged with a Laser scanning confocal microscope (Leica TCS SP5 with LEICA CTR6500 and LAS AF software). In the case of *CaMKIIa*, colocalization ratios for overlapping and non-overlapping probes were 13.7 (±1.6)% and 49.7 (±2.3)%, respectively, and thus very similar to the results obtained with an Axioplan microscope (14.4 (±1.8)% and 51.2 (± 2.4)%). Images were processed with either MetaMorph (only for analysis) or AnalysisB and assembled with Adobe Photoshop CS4, version 11.0 (Adobe). Images were not modified other than adjustments of color, magnification, levels, brightness and contrast.

Supplementary References

Bacci A, Verderio C, Pravettoni E, Matteoli M (1999) Synaptic and intrinsic mechanisms shape synchronous oscillations in hippocampal neurons in culture. *Eur J Neurosci* **11:** 389-397

Dictenberg JB, Swanger SA, Antar LN, Singer RH, Bassell GJ (2008) A direct role for FMRP in activity-dependent dendritic mRNA transport links filopodial-spine morphogenesis to fragile X syndrome. *Dev Cell* **14:** 926-939

Goetze B, Grunewald B, Baldassa S, Kiebler M (2004) Chemically controlled formation of a DNA/calcium phosphate coprecipitate: application for transfection of mature hippocampal neurons. *J Neurobiol* **60:** 517-525

Goetze B, Tübing F, Xie Y, Dorostkar MM, Thomas S, Pehl U, Boehm S, Macchi P, Kiebler MA (2006) The brain-specific double-stranded RNA-binding protein Staufen2 is required for dendritic spine morphogenesis. *J Cell Biol* **172**: 221-231

Papa M, Bundman MC, Greenberger V, Segal M (1995) Morphological analysis of dendritic spine development in primary cultures of hippocampal neurons. *J Neurosci* **15:** 1-11

Rook MS, Lu M, Kosik KS (2000) CaMKIIalpha 3' untranslated region-directed mRNA translocation in living neurons: visualization by GFP linkage. *J Neurosci* **20:** 6385-6393

Tübing F, Vendra G, Mikl M, Macchi P, Thomas S, Kiebler M (2010) Dendritically localized transcripts are sorted into distinct RNPs that display fast directional motility along dendrites of hippocampal neurons. *J Neurosci* **30**: 4160-70

Yuste R, Bonhoeffer T (2001) Morphological changes in dendritic spines associated with long-term synaptic plasticity. *Annu Rev Neurosci* **24:** 1071-1089

Zeitelhofer M, Karra D, Macchi P, Tolino M, Thomas S, Schwarz M, Kiebler M, Dahm R (2008) Dynamic interaction between P-bodies and transport ribonucleoprotein particles in dendrites of mature hippocampal neurons. *J Neurosci* **28:** 7555-7562